The Astrophysical Journal Letters, 989:L32 (9pp), 2025 August 20 https://doi.org/10.3847/2041-8213/adf4e3

Metal-polluted Population III Galaxies and How to Find Them

Elka Rusta[1,2], Stefania Salvadori[1,2], Viola Gelli[3,4], Daniel Schaerer[5], Alessandro Marconi[1,2], Ioanna Koutsouridou[1], and Stefano Carniani[6]
[1] Dipartimento di Fisica e Astronomia, Università degli Studi di Firenze, Largo E. Fermi 1, 50125 Firenze, Italy; elka.rusta@unifi.it
[2] INAF/Osservatorio Astrofisico di Arcetri, Largo E. Fermi 5, 50125 Firenze, Italy
[3] Cosmic Dawn Center (DAWN), Denmark
[4] Niels Bohr Institute, University of Copenhagen, Jagtvej 128, 2200 Copenhagen N, Denmark
[5] Department of Astronomy, University of Geneva, Chemin Pegasi 51, 1290 Versoix, Switzerland
[6] Scuola Normale Superiore, Piazza dei Cavalieri 7, 56126 Pisa, Italy
Received 2025 June 20; revised 2025 July 26; accepted 2025 July 28; published 2025 August 13

Abstract

Observing Population III (hereafter PopIII) galaxies, the hosts of first-generation stars, remains challenging even with the JWST. The current few candidates have been identified through the combination of a prominent He II emission and the absence of metal lines, a well-known but extremely brief signature of metal-free systems. Here, we accurately model the evolution of the emission from PopIII galaxies to increase the number of candidates in JWST observations. To achieve this, we employ a locally calibrated galaxy-formation model that self-consistently follows the star formation and chemical evolution initiated by the first stars. We find that PopIII galaxies can emit metal lines in their "self-polluted" phase, while galaxies host only metal-free stars, but the gas has been chemically enriched by the first supernovae. In this phase, PopIII galaxies have [O III]/H$\beta \approx 1$, which opens the pool of candidates to more easily detectable sources. We predict that the high He II emission of PopIII galaxies can last up to ≈20 Myr and that it is partly maintained in the "hybrid" phase, when PopIII and Population II stars coexist in the host galaxy. We propose novel diagnostics involving ultraviolet metal lines to select PopIII candidates in high-z JWST surveys. In JADES, we identify nine candidate galaxies with >25% of their stellar mass in metal-free stars, showcasing the effectiveness of our method. Ultimately, the key to discovering PopIII galaxies could be to catch them during their first episodes of chemical enrichment.

Unified Astronomy Thesaurus concepts: Population III stars (1285); High-redshift galaxies (734); Chemical enrichment (225); James Webb Space Telescope (2291)

1. Introduction

One of the most ambitious goals of JWST is detecting galaxies that host the first generation of metal-free stars, also known as Population III (hereafter PopIII) galaxies. Despite our current ability to observe the first billion years of the Universe with unprecedented detail, there are only a handful of tentative PopIII candidates (E. Vanzella et al. 2023; R. Maiolino et al. 2024; X. Wang et al. 2024; S. Fujimoto et al. 2025; K. Nakajima et al. 2025). Observing PopIII galaxies is indeed extremely challenging. At high redshifts, $z \approx 30$–15, PopIII galaxies are expected to be the major contributors to the star formation (SF) rate density but to be tremendously faint because of their low stellar masses (e.g, V. Bromm & N. Yoshida 2011; T. Hartwig et al. 2022). As z decreases, PopIII galaxies become brighter but also increasingly rare since they reside in pristine regions of the Universe. Thus, although PopIII galaxies might form down to $z \approx 3$ (e.g., A. Pallottini et al. 2014; B. Liu & V. Bromm 2020; A. Saccardi et al. 2023; O. Zier et al. 2025), to identify them in the plethora of normal (Population II, hereafter PopII) galaxies we need very clear, and long-lasting, spectral signatures.

The search for PopIII galaxies is currently based on the well-established spectral feature of metal-free systems: a strong He II emission combined with the absence of metal lines (e.g., D. Schaerer 2002; A. K. Inoue 2011). While the latter is due to the putative pristine composition of the interstellar medium (ISM) surrounding PopIII stars, the strong He II emission is directly linked to their metal-free nature. Pristine stars are hotter and denser than metal-enriched (PopII) stars, and thus they have harder spectra (e.g., J. Tumlinson & J. M. Shull 2000; P. Marigo et al. 2001). Furthermore, due to the lack of heavy elements in their birth environment, PopIII stars are likely more massive than PopII stars (e.g., J. C. Tan & C. F. McKee 2008; R. S. Klessen & S. C. O. Glover 2023, for a recent review), with simulations predicting initial masses up to $10^3\,M_\odot$ (e.g., S. Hirano et al. 2014; H. Susa et al. 2014) or even more extreme values of $10^5\,M_\odot$ (e.g., T. Hosokawa et al. 2013; D. Nandal et al. 2025). Stellar archeology studies confirm the massive nature of PopIII stars, suggesting a peak of their unknown initial mass function (IMF) of a few tens of solar masses (e.g., M. de Bennassuti et al. 2017; T. Hartwig et al. 2018; G. Pagnini et al. 2023). Since massive stars are intrinsically hotter, a top-heavy PopIII IMF implies an even harder spectrum. Thus, the large amount of energetic radiation produces the strong He II recombination lines that ultimately constitute the clear spectral feature of PopIII galaxies.

Still, only three PopIII candidates have been identified using this key spectral signature: a He II-emitting clump with no associated metal lines at $z = 10.6$ (R. Maiolino et al. 2024), a strong He II emitter at $z = 8.16$ (RX J2129-z8He II, X. Wang et al. 2024), and an extremely metal-poor complex at $z = 6.6$ (LAP1, E. Vanzella et al. 2023; LAP1-B, K. Nakajima et al. 2025). How can we expand the sample of PopIII candidates?

The main challenge in finding PopIII galaxies lies in the brief duration of their key spectral signatures. Indeed, the intensity of the He II recombination lines rapidly decreases after ≈3 Myr (e.g., D. Schaerer 2002). Moreover, the large masses of PopIII stars result in a relatively short lifespan, only ≈(3–30) Myr, after which they quickly pollute the surrounding environment with the metals forged in their brief lifetimes.

PopIII stars ending their life as supernovae (SNe) imprint the surrounding gas with unique abundance patterns (e.g., I. Vanni et al. 2023). These chemical signatures are used to study PopIII–enriched gas in distant absorbers (e.g., U. Maio et al. 2013; I. Vanni et al. 2024) but are neglected when studying the direct emission of PopIII galaxies, typically assumed to host metal-free gas (e.g., E. Zackrisson et al. 2011; J. A. A. Trussler et al. 2023; A. Venditti et al. 2024; M. Lecroq et al. 2025). So far, we lack a comprehensive work that self-consistently combines spectral signatures of metal-free stars with diagnostics of PopIII-polluted gas.

In this Letter, we investigate the evolution of galaxies hosting first-generation stars. To this end, we model their emission spectra throughout different evolutionary phases to understand how long we can still detect the spectral signatures of metal-free stars and address these questions: How does the emission of a PopIII galaxy evolve? Can we detect PopIII stars in a chemically enriched galaxy? How do we identify "hybrid" galaxies that host both metal-free stars and the following metal-enriched generations?

2. Methods

We simulate PopIII galaxies with the locally calibrated galaxy-formation model NEar FiEld cosmology: Re-Tracing Invisible TImes (NEFERTITI; I. Koutsouridou et al. 2023), summarized in Section 2.1. To produce their synthetic emission, we run photoionization models with the Cloudy code (C23 release; G. J. Ferland et al. 1998; M. Chatzikos et al. 2023), as explained in Section 2.2.

2.1. Modeling PopIII Galaxies with NEFERTITI

NEFERTITI is a semianalytical model for the formation and evolution of individual stars in early galaxies, specifically aimed at studying the properties of PopIII stars and their impact on galaxy evolution.

Here we couple NEFERTITI with a dark matter (DM) cosmological simulation of a Milky Way (MW) analog and calibrate it by reproducing a large set of present-day observations for the MW (I. Koutsouridou et al. 2023), including stellar archeology data such as the metallicity distribution function of Galactic halo stars (P. Bonifacio et al. 2021). This calibration is key because the most ancient and metal-poor stars likely formed in the gas enriched by the first PopIII SNe, allowing us to indirectly study PopIII galaxies. For this reason, NEFERTITI is a state-of-the-art model for understanding the evolution of PopIII galaxies.

NEFERTITI grounds on previous semianalytical models (S. Salvadori et al. 2010, 2015) but is specifically designed to explore the unknown PopIII IMF and energy distribution of PopIII SNe (I. Koutsouridou et al. 2023, 2024). Moreover, it employs a random sampling technique to handle weaker SF bursts that cannot fully populate the theoretical IMF in low-mass halos, which is particularly important for PopIII SF. We perform five runs of NEFERTITI with stochastic PopIII IMF sampling and metal enrichment (M. Rossi et al. 2021) to obtain a wide and diverse sample of PopIII galaxies.

At the start of the simulation, NEFERTITI assumes that newly formed DM halos accrete zero-metallicity gas from the intergalactic medium (IGM), with a rate proportional to their DM growth. When the halo mass exceeds a minimum threshold (as in S. Salvadori & A. Ferrara 2009), the first PopIII stars form. The evolution of each star is then tracked individually, following the proper timescale and chemical elements yielded,[7] from C to Zn (I. Koutsouridou et al. 2025). Then, when the ISM metallicity exceeds the critical value, $Z_{\rm gas} > 10^{-4.5}\,Z_{\odot}$ (M. de Bennassuti et al. 2017) normal PopII stars form.

After the SNe explode, part of the ISM metals and gas are injected into the IGM, where the total mass of metals increases over time and so $Z_{\rm IGM} = M_Z^{\rm IGM}/M_{\rm gas}^{\rm IGM}$. To account for the inhomogeneous mixing of metals into the IGM, we use the average evolution of the metal filling factor $Q = V_{\rm fill}/V_{\rm tot}$ computed by S. Salvadori et al. (2014) for MW-like galaxies. At each time step, we randomly assign to a fraction Q of DM halos an enhanced IGM metallicity of $Z_{\rm IGM}/Q$, while the others still accrete pristine gas. With this method, PopIII SF can occur in pockets of pristine gas down to $z \approx 6$.

We adopt a Larson-type IMF, $\phi = {\rm m}^{-2.35}{\rm e}^{(-m_{\rm ch}/M_{\odot})}$ (R. B. Larson 1998), for both PopIII and Population II/I (hereafter PopII/I) stars. We assume that the mass of PopIII stars ranges between $m_{\star} = [0.8,\ 1000]\,M_{\odot}$ and has characteristic mass $m_{\rm ch} = 10\,M_{\odot}$, consistent with stellar archeology constraints (see I. Koutsouridou et al. 2023, 2024). For PopII/I stars we adopt $m_{\star} = [0.1,\ 100]\,M_{\odot}$ and $m_{\rm ch} = 0.35\,M_{\odot}$.

In this Letter, we analyze the evolution from $z = 17$ to $z = 6$ of 1128 PopIII galaxies with total stellar masses $M_{\star} = 10^{2-7}\,M_{\odot}$. At each time step of 1 Myr, we have the following information from NEFERTITI: total stellar/gas/DM mass, stellar population formed, total gas metallicity $Z_{\rm gas}$, gas chemical abundances, and masses of the individual stars formed in each PopIII SF episode.

2.2. Modeling Emission Lines with CLOUDY

We build the stellar emission of PopIII galaxies according to NEFERTITI predictions as follows. For each time step, if the galaxy forms PopIII stars, we sum the emission of individual stars to account for the incomplete sampling of the IMF, using stellar spectra and evolutionary tracks from D. Schaerer (2002). For PopII SF, we adopt an IMF-integrated spectrum, using D. Schaerer (2003) for metal-poor stars ($Z \approx 5 \cdot 10^{-4}\,Z_{\odot}$) and E. Zackrisson et al. (2011) for higher metallicities up to $Z \approx Z_{\odot}$. Then, we assemble the spectra of all the time steps that compose the SF history of the PopIII galaxy up to the desired age (as in E. Rusta et al. 2024).

Then, we input these stellar spectra into the Cloudy photoionization code (M. Chatzikos et al. 2023) to get the total emission of each galaxy. For the gas nebula, we specify the chemical abundances of each element predicted by NEFERTITI, which allows us to follow the metal enrichment of the medium self-consistently. We assume gas clouds with plane-parallel geometry, constant density, no dust, and a

[7] For PopIII stars we assume the yields from A. Heger & S. E. Woosley (2002) and A. Heger & S. E. Woosley (2010), while for PopII stars we assume those of M. Limongi & A. Chieffi (2018).

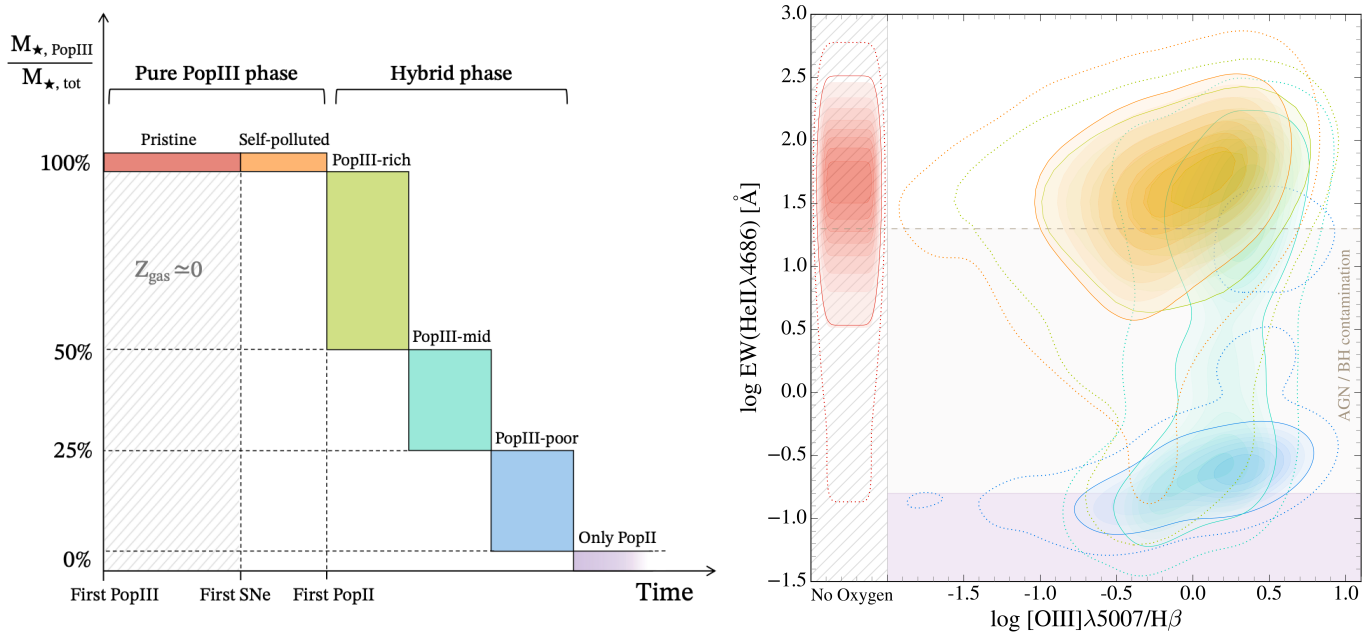

Figure 1. Left: schematic representation of the evolutionary stages of a PopIII galaxy, based on the ratio between PopIII and total $M_\star$. Right: density distributions of NEFERTITI PopIII galaxies on the EW(He IIλ4686) vs. [O III]λ5007/Hβ diagram for log$U = -1$. The colors represent different evolutionary stages, as shown in the left-side scheme. The dotted (solid) lines include 95% (68%) of the population. The horizontal dashed line is the lower limit of the PopIII diagnostic from K. Nakajima & R. Maiolino (2022), with the shaded area below highlighting the AGN and black hole (BH) contamination zone.

fiducial value for the neutral hydrogen density of $10^3\,\mathrm{cm}^{-3}$. For the ionization parameter U, we explore the following wide range of values: log$U = [-3, -2, -1, -0.5, 0]$. The calculations are stopped when the electron fraction falls below 0.01. Ultimately, we have a set of ≈28,000 new photoionization models of PopIII galaxies.

3. Results

We investigate how the emission of a PopIII galaxy evolves in response to the chemical enrichment of its gas and the onset of PopII SF. For this purpose, we explore emission line diagrams involving combinations of He II and metal lines.

3.1. Evolution of a PopIII Galaxy

We begin by identifying the key phases in the evolution of our simulated PopIII galaxies, schematized on the left side of Figure 1. The first is the pure PopIII phase, characterized by a completely metal-free stellar population, and the second is the hybrid phase, in which PopIII stars coexist with PopII stars. These two main stages can be subdivided into more steps. Initially, the galaxy has pristine gas and forms PopIII stars for 3–12 Myr, depending on our stochastic IMF sampling. Then the gas is "self-polluted" by the first PopIII SNe, resulting in a galaxy with a purely metal-free stellar population but chemically enriched gas. In the NEFERTITI model, this phase lasts only for our time resolution of 1 Myr, because the PopIII–enriched gas reaches $Z_{\rm cr}$ and immediately starts forming normal PopII stars. The hybrid galaxy then evolves from a PopIII–rich phase, when $>50\%M_\star$ is metal free, to an intermediate PopIII–mid phase. Then, after 2–5 Myr, it enters into a PopIII–poor phase, when $M_{\star,\rm PopIII} < 25\%M_\star$.

Having determined the main phases of PopIII galaxies, we now study their synthetic emission constructed as described in Section 2.2. Given the rapid enrichment of PopIII galaxies, we choose emission line diagrams that combine characteristic signatures of metal-free and metal-enriched galaxies. The most effective diagnostic of PopIII galaxies is the high equivalent width (EW) of He II lines, especially the optical line at $\lambda = 4686$ Å (K. Nakajima & R. Maiolino 2022; dashed line in the right panel of Figure 1). The nebular oxygen line at $\lambda = 5007$ Å is instead particularly bright in typical star-forming galaxies, with the ratio [O III]λ5007/Hβ (hereafter [O III]/Hβ) being used to determine the gas metallicity (e.g., R. Maiolino & F. Mannucci 2019).

On the right side of Figure 1 we show EW(He IIλ4686) versus [O III]/Hβ for log$U = -1$ (see Appendix A for other U). Our sample of pure PopIII galaxies with pristine gas has predominantly (68% of the total) high EW(He IIλ4686) $\geqslant$4 Å and no oxygen lines. Instead, pure PopIII galaxies with self-polluted gas have the same characteristic He II but simultaneously $0.1 <$ [O III]/H$\beta < 4.5$. This type of emission is maintained in the PopIII–rich phase and, partly, in the PopIII–mid phase. Instead, in the PopIII–poor phase, most galaxies have EW(He II) $<$ 20 Å and are thus populating the region strongly contaminated by active galactic nuclei (AGN) and black holes (K. Nakajima & R. Maiolino 2022). Ultimately, our results show that most galaxies with >50% of their $M_\star$ in metal-free stars, including the pure PopIII ones, have the high EW(He II) $>$ 4 Å expected for pristine stars but also [O III]/H$\beta \geqslant 0.1$, which can be associated with low-Z PopII galaxies.

In Figure 2 we show He IIλ1640/Hβ versus [O III]/Hβ for the same models of Figure 1. Since the ultraviolet (UV) He II line is the key observable used to claim the current PopIII candidates, we report the observations of LAP1-B (K. Nakajima et al. 2025) and RX J2129-z8He II (X. Wang et al. 2024), which have measured Hβ fluxes. To visualize how AGN-like sources contaminate the diagram at high He II/Hβ values, we also report the AGN photoionization models from A. Feltre et al. (2016).

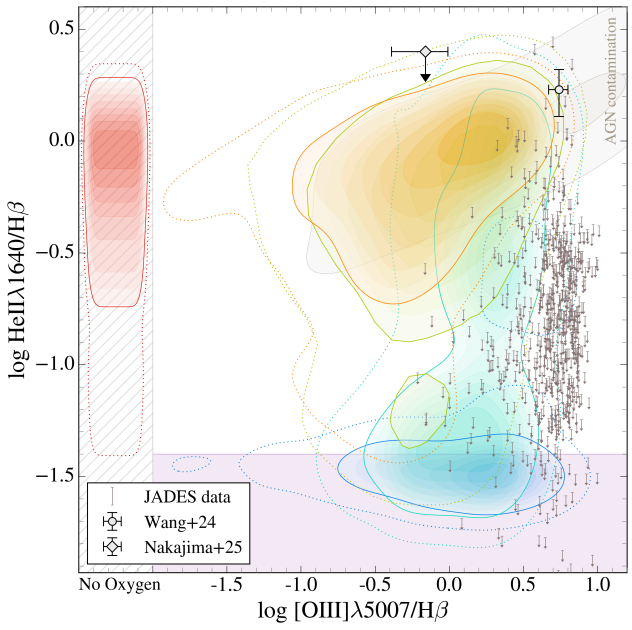

Figure 2. Same as Figure 1 but for He IIλ1640/Hβ vs. [O III]λ5007/Hβ. The gray shaded area represents the region containing 68% of the AGN models from A. Feltre et al. (2016). Points with error bars are observations of LAP1-B (K. Nakajima et al. 2025) and RX J2129-z8He II (X. Wang et al. 2024). The gray arrows are 5σ upper limits from JADES data (F. D'Eugenio et al. 2025).

The emission line ratios of LAP1-B are consistent with our PopIII galaxies, including those with 100% metal-free stars. Still, given the upper limit on the He II line, it remains compatible also with hybrid or PopII galaxies. Moving on to RX J2129-z8He II, it can be reproduced by galaxies that have $M_{\star,\mathrm{PopIII}} > 25\% M_{\star}$, with a higher likelihood for PopIII–rich galaxies. However, the observed [O III]/Hβ is slightly higher than the bulk of our sample, lying in a region where the contamination from AGN is significant.

In the same figure, we report the observed [O III]/Hβ of galaxies from JADES (D. J. Eisenstein et al. 2023; F. D'Eugenio et al. 2025) to showcase how several sources could populate the diagram regions of PopIII galaxies. All the He IIλ1640/Hβ are 5σ upper limits; hence, these galaxies need further observations to determine whether they really are He II emitters and to confirm their PopIII nature using the high EW of He II (Figure 1). Ultimately, our results show that high-z sources should not be excluded as candidate PopIII systems solely based on high [O III] emission, as has been done up to now.

3.2. PopIII Diagnostics: Identifying Candidates

Here, we explore the distribution of PopIII galaxies in diagnostic diagrams involving UV metal emission lines observable at high-z, where we expect to find more PopIII–dominated systems. As outlined in Figure 1, after the initial PopIII phase with pristine gas, PopIII SNe enrich the gas in the galaxies up to $Z_{\mathrm{gas}} = [10^{-4.2}$–$10^{-0.9}]\, Z_{\odot}$ and with a variety of different chemical patterns depending on the progenitor masses and SN explosion energies (e.g., $-1 < [\mathrm{C/O}] < 0.8$, $-7 < [\mathrm{Si/O}] < 0.8$). Thus, we can use metal lines to pinpoint novel PopIII candidates. Hereafter, we will use the following notation: C IVλ1550 (figure) or simply C IV (text) for C IV$\lambda\lambda$1548, 1551, C III]λ1908 or C III] for [C III] λ1907 + C III]λ1909, O III]λ1663 or O III] for O III] $\lambda\lambda$1661, 1666, Si III]λ1888 or Si III] for [Si III] λ1883 + Si III]λ1892, and He II for He IIλ1640.

In Figure 3 we show how our PopIII galaxy models populate UV diagnostic diagrams involving different emission line ratios as a function of C III]/He II, reporting for comparison models for AGN and normal PopII/I star-forming galaxies from A. Feltre et al. (2016) and J. Gutkin et al. (2016). We see that pure self-polluted PopIII galaxies (100% of PopIII stars) are characterized by a low C III]/He II < 0.3, which increases with the decreasing contribution of PopIII stars. However, for different U values, C III]/He II of pure PopIII galaxy models overlaps with that of PopIII–poor models (<25% of M_* in PopIII stars), creating degeneracies. Still, from the left-side diagrams of Figure 3 we can see that the C IV emission strongly depends on U, so its observed value can be used to determine the unknown ionization parameter (Appendix B; see also K. Nakajima & R. Maiolino 2022). Furthermore, if we restrict our analysis to models with $\log U > -2$, which are reasonable for highly ionizing compact sources like PopIII galaxies, we can identify regions that are populated only by models with at least 25% of M_* in PopIII stars, without contamination from AGN or typical SF galaxies. Thus, PopIII galaxy candidates can be spotted by selecting objects that satisfy the following relations:

$$\frac{7}{2}\left(\frac{\mathrm{C\,III]}}{\mathrm{He\,II}}\right)^{-0.3} < \frac{\mathrm{C\,IV}}{\mathrm{C\,III]}} < \frac{5}{2}\left(\frac{\mathrm{C\,III]}}{\mathrm{He\,II}}\right)^{-1.2}, \quad (1)$$

$$\left(\frac{\mathrm{C\,III]}}{\mathrm{He\,II}}\right)^{1.4} < \frac{\mathrm{O\,III]}}{\mathrm{He\,II}} < \frac{1}{2}\left(\frac{\mathrm{C\,III]}}{\mathrm{He\,II}}\right)^{-0.5}, \quad (2)$$

$$\frac{7}{2}\left(\frac{\mathrm{C\,III]}}{\mathrm{He\,II}}\right)^{0.7} < \frac{\mathrm{C\,IV}}{\mathrm{He\,II}} < 2\left(\frac{\mathrm{C\,III]}}{\mathrm{He\,II}}\right)^{-0.3}, \quad (3)$$

$$\left(\frac{\mathrm{C\,III]}}{\mathrm{He\,II}}\right)^{1.3} < \frac{\mathrm{Si\,III]}}{\mathrm{He\,II}} < \frac{1}{8}\left(\frac{\mathrm{C\,III]}}{\mathrm{He\,II}}\right)^{-1.8}. \quad (4)$$

For reference, for $\log U > -2$, C IV and O III] have EW $\sim$ 100 Å, while C III] and Si III] are much less intense, with EW $\sim$ 1 Å (see Appendix C).

In Figure 3, we also include galaxies from the JADES DR3 line flux catalog (F. D'Eugenio et al. 2025). To identify possible candidates, we select JADES galaxies with tentative detections of He II and C IV, lowering the threshold at S/N > 2. We find that nine of the observed galaxies dwell within our novel diagnostics exploiting metal-line ratios for self-polluted PopIII galaxies. These PopIII candidates are also those with the highest He II/Hβ in Figure 2. In particular, one of them has been previously identified as an AGN in J. Scholtz et al. (2025), based on its UV high-ionization lines. However, since this feature is consistent with self-polluted PopIII galaxies, which can have up to [Ne IV]λ2424/C III] λ1909 $\approx$ 1, we still include this object in our PopIII candidate sample.

4. Discussion and Conclusions

The quest for PopIII galaxies, now finally achievable with JWST, has yielded a few promising yet unconfirmed candidates. This scarcity of detections primarily stems from the extremely limited time frame in which we can observe the emission from metal-free environments.

In this Letter, we aimed to increase the number of PopIII candidates by accurately modeling the emission of early

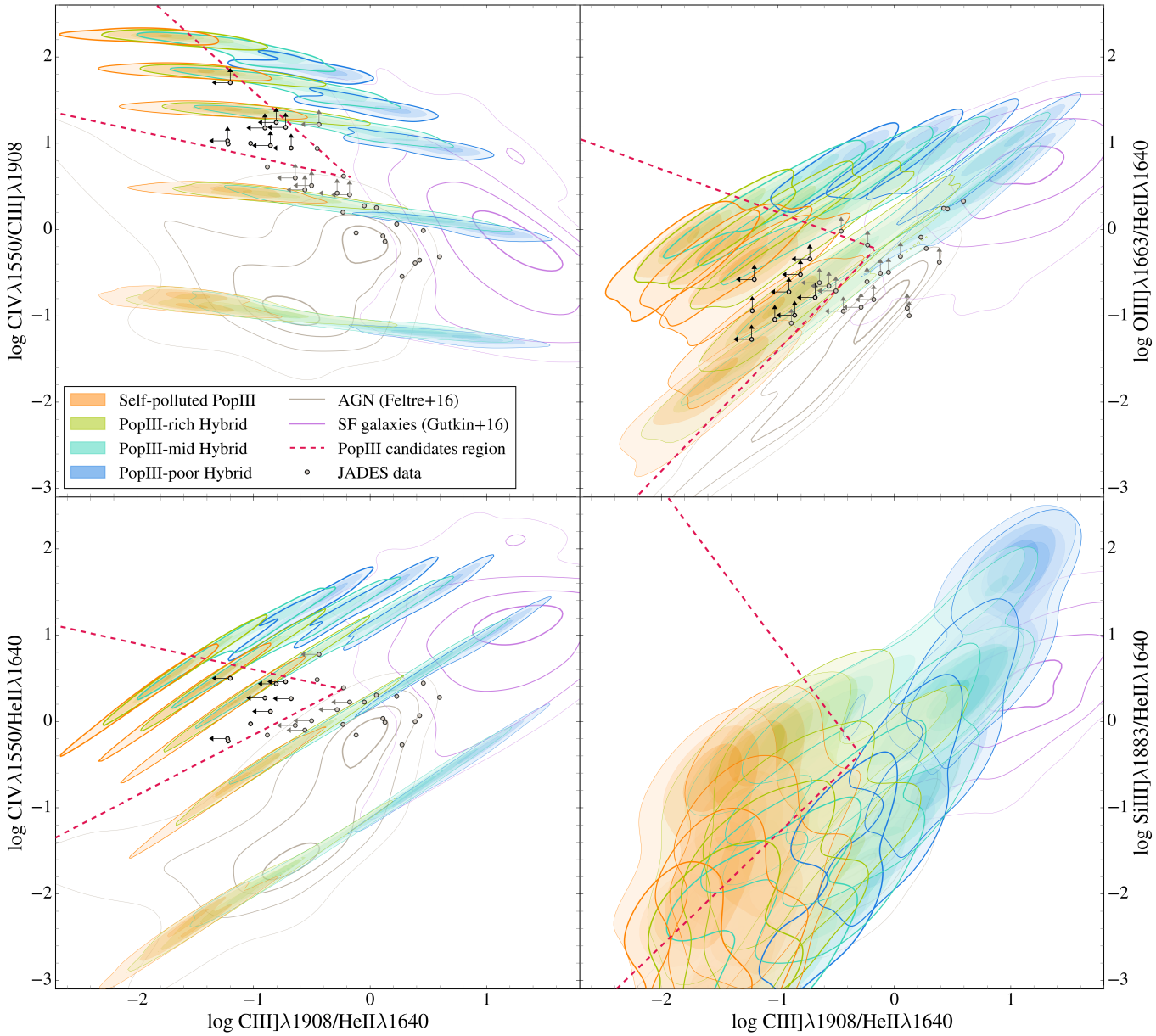

Figure 3. Same as Figure 1 but for different emission line ratios and $\log U = [-3, -2, -1, -0.5, 0]$. The thickness of the contours increases with the U value. The empty contours represent AGN models from A. Feltre et al. (2016; gray) and star-forming galaxy models from J. Gutkin et al. (2016; purple). The red dashed lines are our diagnostics for galaxies with $>25\% M_{\star}$ in PopIII stars (Section 3.2). The gray points are JADES data with tentative He II and C IV detections (S/N > 2), with the darker shade highlighting the sources that we selected as possible PopIII candidates.

galaxies hosting first-generation stars. To this end, we employed NEFERTITI (I. Koutsouridou et al. 2023), a state-of-the-art model for simulating PopIII galaxies, which self-consistently follows the chemical enrichment of their initially pristine gas. The strength of this model is that it is calibrated with numerous local MW observations, including stellar archeology data, but it can also reproduce the properties of MW-like progenitors observed at high-z (E. Rusta et al. 2024).

Our key finding is that pure PopIII galaxies can have metal emission lines due to their self-polluted gas, thus chemically enriched by the first PopIII SNe. Indeed, we find that galaxies with only metal-free stars have [O III]/H$\beta \approx 1$ during their first episodes of metal enrichment, before the onset of PopII formation. This crucial phase can be extended if we consider a temporal delay between PopIII SNe and the subsequent SF, as implemented in other works (e.g., H. Katz et al. 2023). Our finding enlarges the pool of PopIII candidates to include more easily detectable sources with metal emission lines.

Second, we predict that PopIII galaxies can maintain their characteristic high He II emission for up to $\approx$20 Myr, hence not only in their initial pure PopIII stage but also in the following hybrid phase, when PopIII and PopII stars coexist. This is shown in Figure 4, illustrating the results obtained using our NEFERTITI sample of $\approx$1130 PopIII galaxies. If He II/H$\beta > 0.1$, there is $\gtrsim$90% probability that the PopIII galaxy has at least 25% $M_{\star,\mathrm{Pop\ III}}$. Instead, even at high He II/H$\beta > 1$, we can only say that it is a pure PopIII galaxy with 62% probability, but there is still a fair chance that it can be a PopIII–dominated hybrid.

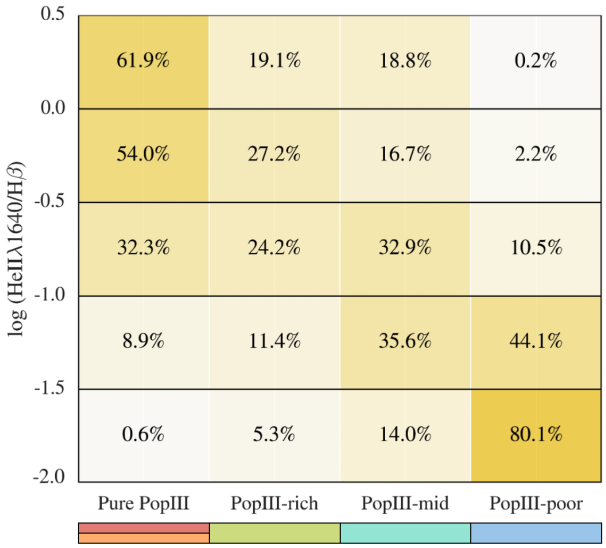

Figure 4. Percentages of NEFERTITI PopIII galaxies in different evolutionary stages (see the left side of Figure 1) as a function of the He II/Hβ emission.

Next, we find that the PopIII candidates LAP1-B (E. Vanzella et al. 2023; K. Nakajima et al. 2025) and RX J2129-z8He II (X. Wang et al. 2024) have He II/Hβ and [O III]/Hβ consistent with our models for PopIII galaxies, including pure self-polluted ones. However, based on these emission line ratios only, we cannot rule out AGN contamination, especially for RX J2129-z8He II.

Finally, we propose novel diagnostics for identifying PopIII candidates at high-z, exploiting UV metal emission lines from PopIII–enriched gas in galaxies that host metal-free stars. We present simple relations between emission line ratios that can help us select pure PopIII and hybrid galaxies with $M_{\star,\mathrm{PopIII}} > 25\% M_{\star}$, without contamination from AGN or PopII/I SF galaxies. However, to discriminate between PopIII stars or intermediate-mass black holes accreting pristine gas, a high EW(He II) is required (K. Nakajima & R. Maiolino 2022).

Among JADES data, we identified nine systems that lie within our new diagnostics and for which we require deep observations to confirm their high He II emission. The number of PopIII candidates found with our proposed method is quite remarkable, considering that we have only used one of the available JWST surveys for high-z galaxies. Thus, this study brings us closer to the long-awaited detection of PopIII galaxies: now we need to observe our candidate sources with the outstanding sensitivity of JWST to confirm their primordial nature.

Acknowledgments

We thank the anonymous referee for their useful and positive comments. This project received funding from the ERC Starting grant NEFERTITI H2020/804240 (PI: Salvadori). A.M. acknowledges support from PRIN-MUR project "PROMETEUS" financed by the European Union—Next Generation EU, Mission 4 Component 1 CUP B53D23004750006, and INAF funding through the "Ricerca Fondamentale 2023" program (mini-grant 1.05.23.04.01).

Appendix A
Ionization Parameter Dependence

In Figure 5 we report the distribution of NEFERTITI PopIII galaxy models for different U values, in the EW(He IIλ4686) versus [O III]/Hβ diagram (top row) and in the He II/Hβ versus [O III]/Hβ diagram (bottom row). We notice that the peaks of the distributions of EW(He IIλ4686) and He II/Hβ remain approximately constant for different U. Instead, the [O III]/Hβ decreases with decreasing U, reducing the likelihood of detecting PopIII galaxies with chemically enriched gas.

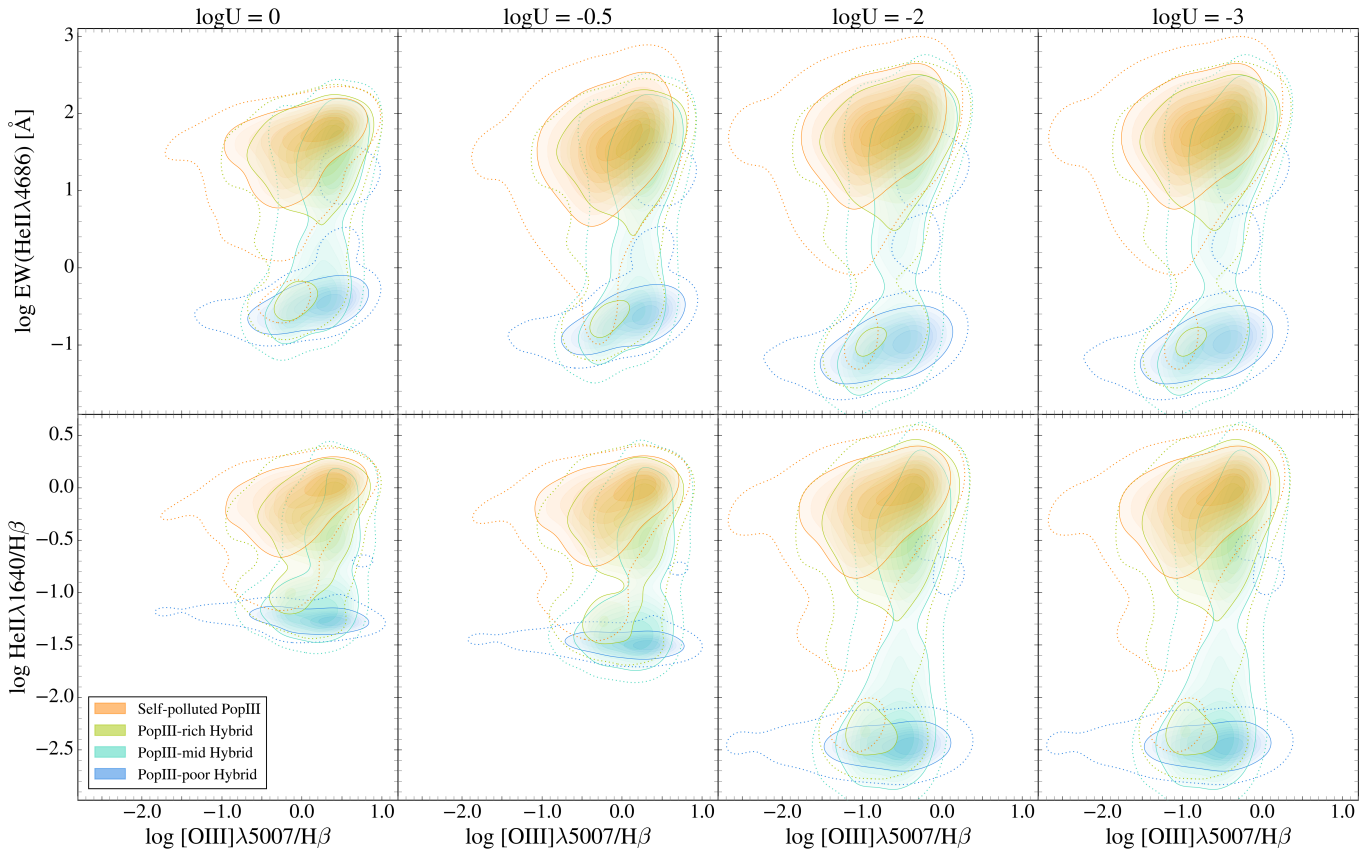

Figure 5. Same as Figure 1 (top row) and Figure 2 (bottom row) but for different U values.

Appendix B
Relations for the Ionization Parameter

Here, we report relations between emission line ratios that can be used as proxies for the unknown U value. Indeed, on the left side of Figure 3, we can identify linear relations for NEFERTITI PopIII galaxy models with fixed U in logarithmic scale:

$$\log(\mathrm{C\,IV}/\mathrm{C\,III}]) = a_1(U) \cdot \log(\mathrm{C\,III}]/\mathrm{He\,II}) + b(U), \quad \text{(B1)}$$

$$\log(\mathrm{C\,IV}/\mathrm{He\,II}) = a_2(U) \cdot \log(\mathrm{C\,III}]/\mathrm{He\,II}) + b(U), \quad \text{(B2)}$$

where the dependence on U can be parameterized as follows:

$$a_1(U) = -0.02 \cdot \log U - 0.24, \quad \text{(B3)}$$

$$a_2(U) = -0.02 \cdot \log U + 0.76, \quad \text{(B4)}$$

$$b(U) = -0.16 \cdot (\log U)^2 + 0.47 \cdot \log U + 1.76. \quad \text{(B5)}$$

Appendix C
EWs of UV Metal Lines

In Figure 6, we report the EWs of C III], C IV, O III], and Si III] versus their ratio with He II. With increasing U, we notice that the EWs of C IV and O III] are higher, while those of C III] and Si III] become lower. Except for C III], the other lines' EWs depend strongly on U, ranging over 4 orders of magnitude. For $\log U > -2$, our PopIII galaxy models have EW(C III]) < 10 Å, EW(C IV) > 10 Å, EW(O III]) > 1 Å, and EW(Si III]) < 30 Å. Moreover, the following condition determines a region populated only by PopIII galaxies with $M_{\star,\mathrm{PopIII}} > 25\% M_\star$:

$$\mathrm{EW}(X) > 10 \cdot X/\mathrm{He\,II}, \quad \text{(C1)}$$

where X represents C IV, C III], O III], or Si III].

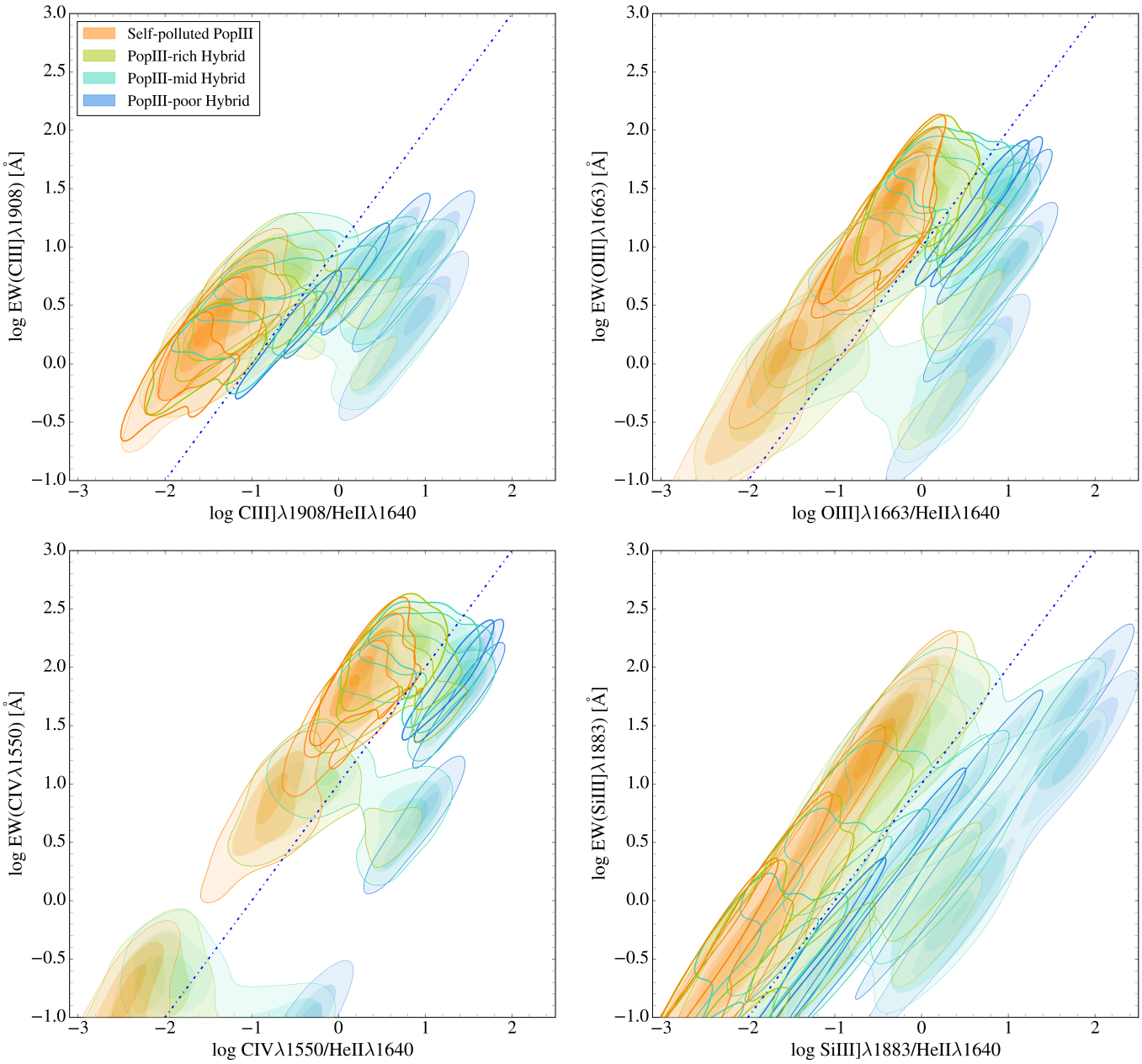

Figure 6. Same as Figure 3 but for the EWs of UV metal lines vs. their ratio with He II. The black dotted lines identify regions populated only by models with >25% PopIII $M_\star$.

ORCID iDs

Elka Rusta https://orcid.org/0009-0006-4326-6097
Stefania Salvadori https://orcid.org/0000-0001-7298-2478
Viola Gelli https://orcid.org/0000-0001-5487-0392
Daniel Schaerer https://orcid.org/0000-0001-7144-7182
Alessandro Marconi https://orcid.org/0000-0002-9889-4238
Ioanna Koutsouridou https://orcid.org/0000-0002-3524-7172
Stefano Carniani https://orcid.org/0000-0002-6719-380X

References

Bonifacio, P., Monaco, L., Salvadori, S., et al. 2021, A&A, 651, A79
Bromm, V., & Yoshida, N. 2011, ARA&A, 49, 373
Chatzikos, M., Bianchi, S., Camilloni, F., et al. 2023, RMxAA, 59, 327
de Bennassuti, M., Salvadori, S., Schneider, R., Valiante, R., & Omukai, K. 2017, MNRAS, 465, 926
D'Eugenio, F., Cameron, A. J., Scholtz, J., et al. 2025, ApJS, 277, 4
Eisenstein, D. J., Willott, C., Alberts, S., et al. 2023, arXiv:2306.02465
Feltre, A., Charlot, S., & Gutkin, J. 2016, MNRAS, 456, 3354
Ferland, G. J., Korista, K. T., Verner, D. A., et al. 1998, PASP, 110, 761
Fujimoto, S., Naidu, R. P., Chisholm, J., et al. 2025, arXiv:2501.11678
Gutkin, J., Charlot, S., & Bruzual, G. 2016, MNRAS, 462, 1757
Hartwig, T., Magg, M., Chen, L.-H., et al. 2022, ApJ, 936, 45
Hartwig, T., Yoshida, N., Magg, M., et al. 2018, MNRAS, 478, 1795
Heger, A., & Woosley, S. E. 2002, ApJ, 567, 532
Heger, A., & Woosley, S. E. 2010, ApJ, 724, 341
Hirano, S., Hosokawa, T., Yoshida, N., et al. 2014, ApJ, 781, 60
Hosokawa, T., Yorke, H. W., Inayoshi, K., Omukai, K., & Yoshida, N. 2013, ApJ, 778, 178
Inoue, A. K. 2011, MNRAS, 415, 2920
Katz, H., Kimm, T., Ellis, R. S., Devriendt, J., & Slyz, A. 2023, MNRAS, 524, 351

Klessen, R. S., & Glover, S. C. O. 2023, ARA&A, 61, 65
Koutsouridou, I., Salvadori, S., & Skúladóttir, Á. 2024, ApJL, 962, L26
Koutsouridou, I., Skúladóttir, Á., & Salvadori, S. 2025, A&A, 699, A32
Koutsouridou, I., Salvadori, S., Skúladóttir, Á., et al. 2023, MNRAS, 525, 190
Larson, R. B. 1998, MNRAS, 301, 569
Lecroq, M., Charlot, S., Bressan, A., et al. 2025, A&A, 695, A17
Limongi, M., & Chieffi, A. 2018, ApJS, 237, 13
Liu, B., & Bromm, V. 2020, MNRAS, 497, 2839
Maio, U., Ciardi, B., & Müller, V. 2013, 435, 1443
Maiolino, R., & Mannucci, F. 2019, A&ARv, 27, 3
Maiolino, R., Übler, H., Perna, M., et al. 2024, A&A, 687, A67
Marigo, P., Girardi, L., Chiosi, C., & Wood, P. R. 2001, A&A, 371, 152
Nakajima, K., & Maiolino, R. 2022, MNRAS, 513, 5134
Nakajima, K., Ouchi, M., Harikane, Y., et al. 2025, arXiv:2506.11846
Nandal, D., Whalen, D. J., Latif, M. A., & Heger, A. 2025, arXiv:2502.04435
Pagnini, G., Salvadori, S., Rossi, M., et al. 2023, MNRAS, 521, 5699
Pallottini, A., Ferrara, A., Gallerani, S., Salvadori, S., & D'Odorico, V. 2014, MNRAS, 440, 2498
Rossi, M., Salvadori, S., & Skúladóttir, Á. 2021, MNRAS, 503, 60264
Rusta, E., Salvadori, S., Gelli, V., Koutsouridou, I., & Marconi, A. 2024, ApJL, 974, L35
Saccardi, A., Salvadori, S., D'Odorico, V., et al. 2023, ApJ, 948, 35
Salvadori, S., & Ferrara, A. 2009, MNRAS, 395, L6
Salvadori, S., Ferrara, A., Schneider, R., Scannapieco, E., & Kawata, D. 2010, MNRAS, 401, L5
Salvadori, S., Skúladóttir, Á., & Tolstoy, E. 2015, MNRAS, 454, 1320
Salvadori, S., Tolstoy, E., Ferrara, A., & Zaroubi, S. 2014, MNRAS, 437, L26
Schaerer, D. 2002, A&A, 382, 28
Schaerer, D. 2003, A&A, 397, 527
Scholtz, J., Maiolino, R., D'Eugenio, F., et al. 2025, A&A, 697, A175
Susa, H., Hasegawa, K., & Tominaga, N. 2014, ApJ, 792, 32
Tan, J. C., & McKee, C. F. 2008, in AIP Conf. Ser. 990, First Stars III, ed. B. W. O'Shea & A. Heger (Melville, NY: AIP), 47
Trussler, J. A. A., Conselice, C. J., Adams, N. J., et al. 2023, MNRAS, 525, 5328
Tumlinson, J., & Shull, J. M. 2000, ApJL, 528, L65
Vanni, I., Salvadori, S., D'Odorico, V., Becker, G. D., & Cupani, G. 2024, ApJL, 967, L22
Vanni, I., Salvadori, S., Skúladóttir, Á., Rossi, M., & Koutsouridou, I. 2023, MNRAS, 526, 2620
Vanzella, E., Loiacono, F., Bergamini, P., et al. 2023, A&A, 678, A173
Venditti, A., Bromm, V., Finkelstein, S. L., et al. 2024, ApJL, 973, L12
Wang, X., Cheng, C., Ge, J., et al. 2024, ApJL, 967, L42
Zackrisson, E., Rydberg, C.-E., Schaerer, D., Östlin, G., & Tuli, M. 2011, ApJ, 740, 13
Zier, O., Kannan, R., Smith, A., et al. 2025, arXiv:2503.03806